Density of discrete levels in ^{116}Sn

A. V. Ignatyuk* and J. L. Weil
University of Kentucky, Lexington, Kentucky 40506

S. Raman and S. Kahane†
Oak Ridge National Laboratory, Oak Ridge, Tennessee 37831

(Received 12 November 1992)

Model fits were made to the cumulative distribution of all known levels (with spins $J \leq 10$) in ^{116}Sn below an excitation energy of 4.1 MeV identified in a variety of experiments, and simultaneously to the density of $J=0$ and $J=1$ resonances inferred from neutron capture and total cross-section measurements in ^{115}Sn+n. Neither the back-shifted Fermi-gas model nor the constant-temperature model provides a satisfactory fit over the entire energy range. The generalized superfluid model, with a level-density parameter and spin-cutoff factor that are both energy dependent, does give a good fit, and the resulting best-fit parameter values are consistent with those found in other applications of this model.

PACS number(s): 21.10.Ma, 27.60.+j

I. INTRODUCTION

The densities of excited nuclear levels have been a matter of concern and study for over 50 years going back at least to 1936 when the Fermi-gas model (FGM) was put forth by Bethe [1]. Ericson [2] realized 30 years ago that there was difficulty in fitting the densities of both low-lying bound states and high-lying unbound states (in the neutron resonance region) with the FGM, which, for fundamental reasons, was thought to be applicable only to the higher-energy regions. At that time it was believed that the constant-temperature model (CTM) [2,3] could give a good representation of the experimental data below the neutron separation energy (S_n). An analysis by Gilbert and Cameron [4] attempted to treat the two regions separately with these two models, with an *ad hoc* method of joining the two level-density curves tangentially at some point determined by the available data and systematics. The Gilbert and Cameron procedure contained four parameters and was considered cumbersome by many users who, therefore, preferred the back-shifted Fermi-gas model (BSFGM) [5] with only two parameters. A practical set of parameters was supplied by Dilg *et al.* [6], who analyzed the level densities of 220 nuclei by fitting the BSFGM two-parameter formula to two data points for each nucleus, namely, the cumulative number of bound states at some energy and the density of s-wave resonances at S_n. More recently, von Egidy, Bekhami, and Schmidt [7,8] have concluded, on the basis of fits to all known bound levels up to a certain energy and to the resonance-region level densities of 87 nuclei, that both the BSFGM and the CTM formulas work equally well in reproducing experimental densities. The predictive power of the parameters supplied in Ref. [8] is tested here in the case of ^{116}Sn.

A nearly "complete" level scheme (see Table V of Ref. [9]) for the bound states of ^{116}Sn up to an excitation energy of 4.3 MeV has recently been established from detailed studies of the ^{116}Sn$(n,n'\gamma)$ and the ^{115}Sn(n,γ) reactions combined with all previous studies of levels in this nucleus. This scheme consists of 81 levels up to 3.9 MeV and 112 levels up to 4.3 MeV. The density of s-wave resonances (at $S_n=9562$ keV) has also recently been inferred as $\rho(S_n)=21\,700\pm6600$ MeV^{-1} [10]. It is now possible to test, over an extended excitation energy region in ^{116}Sn, the ability of various models to simultaneously fit the densities of both bound and unbound states.

This paper is organized as follows. Section II presents the results of fits using either the BSFGM or the CTM; these fits are relatively poor when compared to the data over the entire energy range. As shown in Sec. III, better fits were obtained to the same data with the phenomenological version [11,12] of the more recent generalized superfluid model (GSM) [13,14]. In Sec. IV, the data are also compared to a microscopic calculation with this newer model. The conclusions are given in Sec. V. The expressions needed for the calculation of the level density, taking into account the shell model, collective, and superfluid effects, are given in the Appendix.

The three level-density expressions considered here are sufficiently similar that a less than perfect fit, suitable for most practical applications, can be achieved with any one of them *if* the data are readily available. The differences then lie in the details. Obviously, the utility of a model is greatly enhanced if it has correct predictive powers. Despite five decades of effort, the respective model parameters have not been established precisely enough, from either global systematics or theory, that predictions of level densities can be made *a priori* in a reliable fashion over an extended energy region for a given nucleus. Studies similar to that reported here help establish these parameters.

*Permanent address: Institute of Physics and Energy, Obninsk, Russia.

†Permanent address: Nuclear Research Centre-Negev, Beer-Sheva, Israel.

II. FERMI-GAS AND CONSTANT-TEMPERATURE MODELS

A. BSFGM formulas and fits

The first model tested was the back-shifted Fermi-gas model, which has been used before in several global analyses of experimental data (see, for example, Refs. [6–8]). In the fits discussed below, it was assumed that the level scheme for ^{116}Sn is complete up to an excitation energy of 3.9 MeV, and possibly 4.1 MeV. The total number N of bound states up to 3.9 MeV, $N(3.9)$, is 81; $N(4.1)=97$; and $N(4.3)=112$. There are definite indications that levels are being missed above 4.1 MeV. All three upper limits (3.9, 4.1, and 4.3 MeV) were used in the fitting procedure. The influence of the nine lowest-lying levels was also tested by fitting with and without them, on the grounds that a statistical model does not pretend to describe these levels. The conclusions drawn are valid regardless of which subset of levels was included in the fit.

Following von Egidy, Bekhami, and Schmidt [7,8], the formula for the level density (in units of MeV^{-1}) of the BSFGM,

$$\rho(U,J,\pi)=\frac{\exp\{2\sqrt{[a(U-E_1)]}\}f(J)}{24\sqrt{2}\sigma a^{1/4}(U-E_1)^{5/4}}\ , \tag{1}$$

was used, where U is the excitation energy, E_1 the energy shift parameter, and a the level-density parameter. If unequal parity ratios can be ignored,

$$\rho(U,J,\pi)=\tfrac{1}{2}\rho(U)f(J)\ . \tag{2}$$

The distribution of spins J for the excited levels is given by [4]

$$f(J)=e^{-J^2/2\sigma^2}-e^{-(J+1)^2/2\sigma^2}$$
$$\approx\frac{2J+1}{2\sigma^2}\exp[-(J+\tfrac{1}{2})^2/2\sigma^2]\ , \tag{3}$$

where σ^2 is the spin-cutoff parameter, which may be energy dependent. The thermodynamic temperature t is defined by (see Eq. (9) of Ref. [5])

$$U-E_1=at^2\ . \tag{4}$$

The staircase plot of the cumulative number of bound states (see Fig. 1) and the neutron-resonance density were fit simultaneously with Eq. (1) and its integral. The least-squares-fitting procedure was similar to procedure A described in Ref. [7]. Basically, the χ^2 value defined by

$$\chi^2=\left[\frac{\rho_{\rm expt}-\rho_{\rm calc}}{\Delta\rho_{\rm expt}}\right]^2+\sum_i\left[\frac{N(E_i)-i}{\sqrt{i}}\right]^2 \tag{5}$$

is minimized. In Eq. (5), $\rho_{\rm expt}$ and $\rho_{\rm calc}$ are, respectively, the experimental and calculated density of $J=0$ and 1 states (of both parities) at S_n, and $N(E_i)$ is the integrated level density up to level i. The values of a and E_1 were kept close to those recommended by von Egidy, Schmidt, and Bekhami [8] on the basis of their global survey.

The density $\rho(S_n)$ of s-wave neutron resonances at S_n (which is the measured quantity that is usually tabulated) is not known directly, but has been inferred [10] from a Hauser-Feshbach-Moldauer analysis of neutron capture data in the 20–450-keV region and total neutron cross-section data in the 20–1400-keV region. The inferred value of 21 700±6600 MeV^{-1} is fairly reliable because data on 10 stable isotopes of tin were analyzed in an internally self-consistent manner. In particular, for those tin isotopes for which directly measured values are available [15], the inferred densities are consistent with measurements. The weight for this datum was taken as $\frac{1}{10}$ the experimental uncertainty to force better agreement with this data point, but the full uncertainty was taken into account in determining the uncertainties in the fitted values. Essentially the same results were obtained using both a $(1.5)^{-1}$ (see Ref. [7]) and a $(\sqrt{i}\,)^{-1}$ weighting factor for the bound states, where i is the index of the ith level. The latter was used to give sufficient relative weight to the more widely spaced levels at low excitation. The energy-independent value of σ^2 was taken from Eq. (3) of Ref. [8].

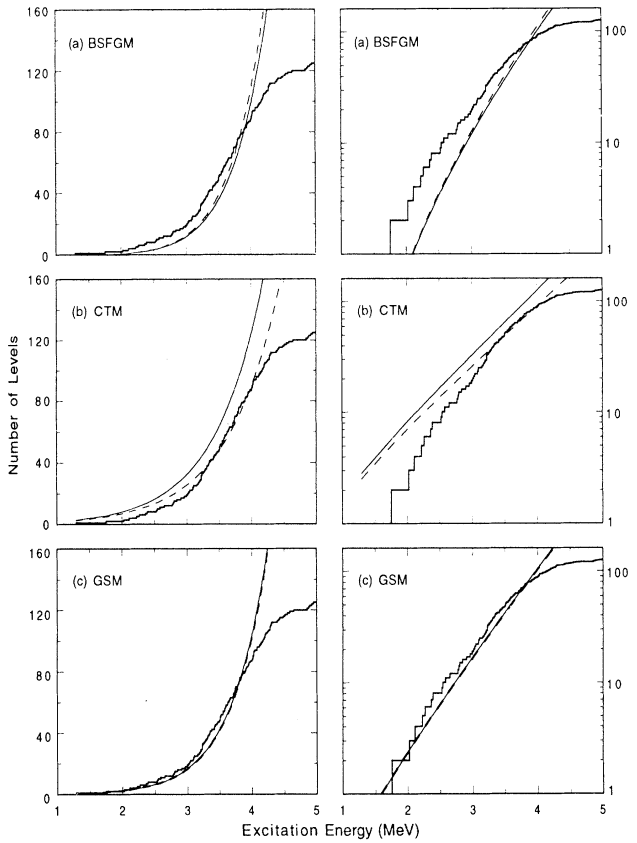

FIG. 1. Staircase plot, based on Table V of Ref. [9], of the cumulative number of levels N as a function of excitation energy. The solid curves are least-squares fits with different models [(a) back-shifted Fermi-gas model, (b) constant-temperature model, and (c) generalized superfluid model] to this data (in the region 2.5–4.1 MeV) and to the density of $J=0$ and 1 states just above the neutron separation energy (9.562 MeV). The dashed curves are fits to the bound states alone. The same information is shown twice; with a linear ordinate on the left and logarithmic on the right. See also Table I.

For illustrative and testing purposes, E_1 was set equal to 1.55 MeV [deduced from the C_1 value given by Eq. (10) of Ref. [8] and Δ(pairing)=2.996 MeV], and a search was made to find the best a value. The results with a $(\sqrt{i}\,)^{-1}$ weighting factor are shown by the solid (with resonances) and dashed (without) curves in Fig. 1(a), and are also given in Table I. The fitted values (in MeV^{-1}) of 12.8 (with resonances) and 13.0 (without) are consistent with 13.1 from systematics [8]. However, it can be seen from this figure that the fit is poor in the 2.5–4.1-MeV bound-state region.

B. CTM formula and fits

The bound states alone and the bound states plus resonance density were also fit with the constant-temperature model formula relating the nuclear temperature T (which is different from the thermodynamic temperature t [see Eq. (4)]) to the level density

$$\rho(U)=\frac{1}{T}\exp\left[\frac{(U-E_0)}{T}\right]. \tag{6}$$

This formula has long been known [2-4] to provide a reasonably good fit to the low-lying bound states. The results are shown in Fig. 1(b). The parameters of the fit along with the level density in the resonance region calculated from these parameters are given in Table I. The value of E_0 was set at 0.37 MeV; this central value was based on the C_0 value given by Eq. (10) of Ref. [8] and Δ(pairing)=2.996 MeV. The fitted T values of 0.77 and 0.81 MeV are again close to 0.75 MeV from systematics [8]. While the fit (dashed curve) to the bound states alone seems to be quite good, the density at S_n is now underestimated by a factor of 3–4. Forcing agreement at S_n results in a poor fit (solid curve) for the bound states [see Fig. 1(b)]. However, this fit can be improved, as shown later in Fig. 3(b), by changing E_0.

All the previous conclusions are consistent with the discussions found in Ref. [4] and in other more recent analysis [16]. To calculate the level density in the energy gap between the known bound-state cluster of levels and S_n—a region in which it is very difficult to be certain that all levels of specified J^π values have been identified experimentally, not to mention all levels with all permissible J^π values—Gilbert and Cameron [4] suggested an *ad hoc* method of joining the results of the CTM and the FGM. The prescription for obtaining a level-density relation with the appropriate continuity properties is discussed at some length in their paper and also in Ref. [16]. On the other hand, von Egidy, Bekhami, and Schmidt [7,8] have concluded that *both* level-density formulas appear to fit the two energy regions equally well for 87 nuclei in the mass range $20 \leq A \leq 250$. If true, either formula is a valid representation for bridging this energy gap and can be employed safely in many applications that require a good level-density formula as input. However, in their analysis, the number of bound states (in an even-even nucleus) exceeded 44 (45% of the number in the current analysis) in only two cases (^{158}Gd and ^{168}Er), and in both cases the upper energy limit for the bound states, 2.1 MeV, was only ~50% of the current case (4.1 MeV). (As a fairer comparison, the upper energy limits of the

TABLE I. Best-fit parameters from least-squares fits with the back-shifted Fermi-gas model (BSFGM) and the constant-temperature model (CTM). The fitted data are the 97 bound states in ^{116}Sn below 4.1 MeV (from Table V of Ref. [9]) minus the first nine levels up to 2.5 MeV. Fits were made with and without the information on the density ρ of s-wave neutron resonances at the neutron separation energy S_n. The BSFGM has two parameters a and E_1 [see Eq. (1)]. The CTM also has two parameters E_0 and T [see Eq. (5)]. The spin-cutoff parameter σ^2 of Eq. (3) was taken as 15.1 from Ref. [8]. The quoted uncertainties in the a and T values and the ranges of χ^2 and $\rho(S_n)$ are derived from attempting similar fits to 81 bound states below 3.9 MeV and 112 below 4.3 MeV while also taking into account, where necessary, the uncertainty in the density of resonances.

Source	Resonances	a (MeV^{-1})	E_1 (MeV)	E_0 (MeV)	T (MeV)	χ^2	$\rho(S_n)$(MeV^{-1})
Experiment							21 700 ± 6 600
BSFGM	yes	$12.8^{+0.3}_{-0.4}$	1.55[a]			230 – 490	17 000 – 28 300
BSFGM	no	13.0 ± 0.6	1.55[a]			95 – 455	18 000 – 38 000
CTM	yes			0.37[a]	0.77 ± 0.01	600 – 1 300	14 300 – 18 700
CTM	no			0.37[a]	0.81 ± 0.01	60 – 80	5 500 – 7 000

[a]Value recommended in Ref. [8]. Fits were also made with E_1 and E_0 values that fall within the bounds given in Ref. [8].

known bound states in the analyses of ^{158}Gd, ^{168}Er, and ^{116}Sn represent 35, 27, and 43 %, respectively, of the corresponding S_n values.) For the specific case of ^{116}Sn, it can be concluded from Fig. 1 and Table I that, while staying within the bounds of previously established systematics, it is difficult, if not impossible, to either extrapolate the BSFGM down from the resonance region to fit the bound states or extrapolate the CTM up from the bound states to reproduce correctly the level density in the resonance region. Two-parameter BSFGM fits, with and without resonances, were consistently below the bound-state data, and the CTM fits were above.

III. GENERALIZED SUPERFLUID MODEL

A. Introduction

The CTM and the FGM are simple models that were first put forward many decades ago when nuclear physics was in its infancy. They ignore concepts such as pairing correlations, shell effects, and collectivity, all of which were introduced in later years. All three of these concepts have been incorporated into the generalized superfluid model, which has been developed over the last 20 years [13,14]. For easy comparison to experimental data, a phenomenological version of this model was put forward by Ignatyuk and co-workers [11,12]; this version is now applied for the analysis of the ^{116}Sn data.

To take pairing correlations and collective effects into account, it is necessary to use in Eq. (2) the following expression for the total level density:

$$\rho(U)=\rho_{\rm qp}(U')\kappa_{\rm vibr}(U')\kappa_{\rm rot}(U') , \tag{7}$$

where the effective excitation energy U' is defined below. The quantity $\rho_{\rm qp}(U)$ is the level density of quasiparticle excitations in a Bardeen-Cooper-Schrieffer- (BCS) type theory, which includes pairing correlations that produce the superfluid characteristics of this model. The quantity $\kappa_{\rm vibr}(U)$ takes into account the collective enhancement of the level density resulting from vibrational excitations. The rotational enhancement factor $\kappa_{\rm rot}(U)$ was set to unity because ^{116}Sn is a spherical nucleus. The expressions needed to calculate $\rho_{\rm qp}(U)$, $\kappa_{\rm vibr}(U)$, and $\kappa_{\rm rot}(U)$ are given in the Appendix.

The influence of pairing correlations on the level density is a function of the thermodynamic temperature t. One of the basic parameters of the GSM is the pairing-correlation function Δ_0, which is directly related to the critical temperature $t_{\rm cr}$ (of the phase transition from the superfluid state to the normal state) by [11,12]

$$t_{\rm cr}=0.567\Delta_0 . \tag{8}$$

Above $t_{\rm cr}$, the energy dependence of the GSM level density differs from that of the BSFGM by a shift of the excitation energy, as given in Eqs. (A2) and (A6) of the Appendix. Below $t_{\rm cr}$, this energy dependence is similar to that of the CTM.

To account for possible deficiencies in the global parametrization of the collective enhancement factors and pairing correlation functions, an additional shift in the excitation energy, $\delta_{\rm shift}$, was added to the phenomenological GSM [12]. The excitation energy U' of Eq. [7] is defined as[1]

$$U'=U+n\Delta_0+\delta_{\rm shift} , \tag{9}$$

where U is the true excitation energy of the nucleus, $n=0$, 1, or 2 for even-even, odd, or odd-odd nuclei, respectively, and $\delta_{\rm shift}$ is discussed again below.

The main difference between the normal and superfluid phases is connected with their differing spectra of quasiparticle excitations. In the normal phase, the quasiparticle energies are given by

$$E_{\rm qp}=|E_{\rm sp}-E_F| , \tag{10a}$$

where $E_{\rm sp}$ and E_F are the single-particle and Fermi energies, respectively. In the superfluid phase, the quasiparticle energies are given by

$$E_{\rm qp}=\sqrt{(E_{\rm sp}-E_F)^2+\Delta_0^2} . \tag{10b}$$

These differences strongly affect all thermodynamic properties of the nucleus, and, hence, the level density.

B. GSM formulas and fits

In the GSM, the effects of nuclear shell structure cause a to have an *energy dependence* given by

$$a(U,Z,A)=\begin{cases}\tilde{a}(A)\left\{1+\dfrac{[f(U'-E_{\rm cond})\delta\varepsilon_0(Z,A)]}{(U'-E_{\rm cond})}\right\} & \text{for } U'\geq U_{\rm cr} ,\\ a_{\rm cr} \quad \text{for } U'<U_{\rm cr} .\end{cases} \tag{11}$$

Here $\tilde{a}(A)$ is the asymptotic value of a at high excitation energy; the dimensionless function $f(U)$ determines the energy behavior of a at lower excitation energies; the condensation energy $E_{\rm cond}$ is defined by Eq. (A6) of the Appendix; and $\delta\varepsilon_0(Z,A)$ is the shell correction in the nuclear binding energy. The method for determining $U_{\rm cr}$ corresponding to $t_{\rm cr}$ is described in the Appendix; for ^{116}Sn, $U_{\rm cr}\approx 6$ MeV. The function $f(U)$ has the form [11,12]

$$f(U)=1-\exp(-\gamma U), \tag{12}$$

[1] In Ref. [11], U' was given incorrectly as $U'=U-n\Delta_0+\delta_{\rm shift}$.

where

$$\gamma = 0.40 A^{-1/3} \text{ MeV}^{-1} \quad (13)$$

is given by both the theoretical predictions of the changes in the level-density parameters and the analyses of experimental data [12,17]. For ^{116}Sn, the shell correction $\delta\varepsilon_0 = -0.59$ MeV (see Ref. [18]) is relatively small, and the energy dependence of the level-density parameter a is not very pronounced. Note that $a(U,Z,A) = a_{cr}$ = a constant for $U' \leq U_{cr}$.

The current version of the phenomenological GSM has three parameters $\tilde{a}(A)$, Δ_0, and δ_{shift}. For $A \geq 50$, two of the three parameters can be determined fairly well from either systematics or theory and can be evaluated from the expressions [11,12]

$$\tilde{a}(A) = (0.073A + 0.115A^{2/3}) \text{ MeV}^{-1} \quad (14)$$

and

$$\Delta_0 = 12 A^{-1/2} \text{ MeV} . \quad (15)$$

The third parameter, δ_{shift}, is an *ad hoc* supplementary shift of the excitation energy often needed to simultaneously describe well [12] the density of low-lying levels and of neutron resonances. Generally, away from doubly magic nuclei, δ_{shift} is ~ 0.5 MeV. This value and the $\tilde{a}(A)$ and Δ_0 values given by Eqs. (14) and (15) are useful as starting values to limit the possible meanderings during a multiparameter least-squares search.

As before, the fit to the 2.5–4.1-MeV bound-state data was carried out to the cumulative number of levels, while at S_n it was twice the density of s-wave neutron resonances, $\rho_{expt} = 2\rho(S_n)$, that was fitted. In fitting the experimental data, various combinations of one, two, and three parameters were varied in order to test for the range and stability of the best-fit parameter values. A $(\sqrt{i})^{-1}$ weighting factor was used for the bound states and a factor of $\frac{1}{10}$ the experimental uncertainty for the unbound states, just as in the previous fits. Because these weights do not reflect true experimental uncertainties, the resulting χ^2 values have only relative significance, similar to the situation in Refs. [7,8].

With $\Delta_0 = 1.114$ from systematics [see Eq. (15)], the parameters $\tilde{a}(A)$ and δ_{shift} were found to be closely coupled, and the value of $\tilde{a}(A)$ could not be determined unambiguously unless the resonance region was included in the fit or δ_{shift} was constrained. Typical results of least-squares fits to the bound states of ^{116}Sn below 4.1-MeV excitation energy, with or without the inclusion of the resonances, are shown in Fig. 1(c). The best-fit values of $\tilde{a}(A)$ and δ_{shift} along with the calculated density of s-wave resonances are given in Table II. The $\tilde{a}(A)$ values are somewhat higher than the systematics value of 11.2 given by Eq. (14), but the fits of Grudzevich *et al.* [12] to both bound-state and neutron-resonance densities of more than 80 nuclei show similar high values of $\tilde{a}(A)$ for nuclei in the tin region. Figure 1 and Tables I and II show that the GSM is more successful in reproducing the experimental data in the 1–4-MeV region than either the BSFGM or the CTM.

When the total number of known bound states in a medium-weight or heavy nucleus is large (say >50), a spin and parity (J^π) assignment is usually not available for each and every level. The nucleus under study, ^{116}Sn, is atypical in that a preferred J^π value is listed in Table V of Ref. [9] for each of the 112 levels below 4.3 MeV. As an additional check of the consistency of the GSM, the distribution of the experimentally determined spins was used for the determination of the spin-cutoff parameter (see Fig. 2). For the 1.5–2.5-MeV interval, the six known levels imply $\sigma^2 = 5.3 \pm 1.5$, and for the 2.5–3.9-MeV interval, $\sigma^2 = 11.4 \pm 1.5$. Both values differ

TABLE II. Best-fit parameters from least-squares fits with the generalized superfluid model (GSM). The fitted data are the 97 bound states in ^{116}Sn below 4.1 MeV (from Table V of Ref. [9]) minus the first nine levels up to 2.5 MeV. Fits were made with and without the information on the density ρ of s-wave neutron resonances at the neutron separation energy S_n. The GSM has three parameters $\tilde{a}(A)$, Δ_0, δ_{shift} [see Sec. III.B]. The spin-cutoff parameter σ^2 of Eq. (3) is given by Eqs. (A.2) and (A.3). The quoted uncertainties in the a and T values and the ranges of χ^2 and $\rho(S_n)$ are derived from attempting similar fits to 81 bound states below 3.9 MeV and 112 below 4.3 MeV while also taking into account, where necessary, the uncertainty in the density of resonances.

Source	Resonances	$\tilde{a}(A)$ (MeV^{-1})	Δ_0 (MeV)	δ_{shift} (MeV)	χ^2	$\rho(S_n)$(MeV^{-1})
Experiment						21 700 ± 6 600
GSM	yes	$12.9^{+0.9}_{-1.2}$	1.114[a]	$0.67^{+0.07}_{-0.09}$	20 – 310	14 900 – 28 200
GSM	no	$12.7^{+1.2}_{-1.6}$	1.114[a]	0.67[b]	25 – 255	11 100 – 30 200

[a]From Eq. [15].

[b]Held fixed because of the close coupling between δ_{shift} and $\tilde{a}(A)$ when fitting only bound states. See Sec. III.B.

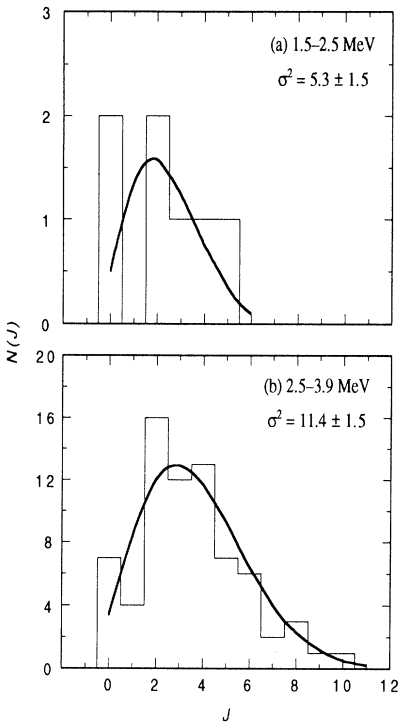

FIG. 2. Spin-cutoff factors σ^2 for the (a) 1.5–2.5-MeV and (b) 2.5–3.9-MeV energy intervals deduced from fits of Eq. (3) to the number $N(J)$ of levels with a particular spin (J) value (data from Table V of Ref. [9]) in that interval.

significantly from the energy-independent spin-cutoff parameters $\sigma^2=18.8$ and 15.1 given by Eq. (17) of Ref. [7] and Eq. (3) of Ref. [8], respectively.

The analyses until now ignore parity. However, Table V of Ref. [9] shows that the parity distribution is clearly lopsided with 86 $\pi=+$ and 26 $\pi=-$ states in ^{116}Sn below 4.3 MeV. (Presumably the numbers of positive- and negative-parity states with the same spin will become equal at the neutron separation energy and at higher excitation energies; at any rate such an assumption is implicit in the models considered here.) As an exercise in dealing with this unequal parity ratio, fits were made in the energy range up to 4.1 MeV to the $\pi=+$ levels alone and to the $\pi=-$ levels alone. The results of these fits are given in Table III. As expected, the average of the respective parameters from the fitting of the positive- and the negative-parity levels separately is very close to the parameters for fitting all the levels together.

Even though two parameters are involved, the fits shown in Figs. 1(a) and 1(b) are single-parameter fits because E_1 in the case of the BSFGM and E_0 in the case of the CTM were constrained, for testing purposes, to the values recommended in Ref. [8]. The fits shown in Fig. 3 are genuine two-parameter fits to the bound states plus resonances for all three models and represent the best that can be currently achieved. Figure 3(b) and the relative χ^2 values (in parentheses) for the BSFGM (175), CTM (470), and GSM (90) establish that the GSM fit is clearly superior over the whole 1–4-MeV range. The calculated $\rho(S_n)$ values of 21 400 (BSFGM), 21 100 (CTM), and 21 600 (GSM) are nearly the same, but the cumulative number of levels predicted at S_n [see Fig. 3(a)] are different mainly because the spin-cutoff parameter σ^2 in $\rho(U,J)$ is different among the GSM, on the one hand, and the BSFGM and CTM on the other [see Fig. 4(a)].

The comparison of the experimental spin-cutoff parameters with those calculated in the phenomenological GSM [see Eqs. (A2) and (A3)] is shown by the dashed curve in Fig. 4(a). This model gives approximately the same increasing slope with energy as found experimentally, but the absolute value is a little higher. Possible reasons for this difference are discussed in the next section.

TABLE III. Best-fit parameters from least-squares fits with the generalized superfluid model (GSM). The fitted data are $\rho(S_n)$ representing the $J=0$ and $J=1$ states of either parity at the neutron separation energy S_n and (a) only the 74 positive-parity states (b) only the 23 negative-parity states, and (c) all 97 bound states in ^{116}Sn below 4.1 MeV minus the first seven positive-parity and two negative-parity levels. The GSM has three parameters $\tilde{a}(A)$, Δ_0, δ_{shift} [see Sec. III.B]. The spin-cutoff parameter σ^2 of Eq. (3) is given by Eqs. (A.2) and (A.3).

Source	Parity	$\tilde{a}(A)$ (MeV^{-1})	Δ_0 (MeV)	δ_{shift} (MeV)	χ^2	$\rho(S_n)$ (MeV^{-1})
Experiment						21 700 ± 6 600
GSM (a)	Positive only	12.1	1.114[a]	0.90	40	21 650
GSM (b)	Negative only	13.8	1.114[a]	0.42	10	21 700
GSM	Average	13.0	1.114[a]	0.66		21 675
GSM (c)	Both	12.9	1.114[a]	0.67	90	21 600

[a]From Eq. [15].

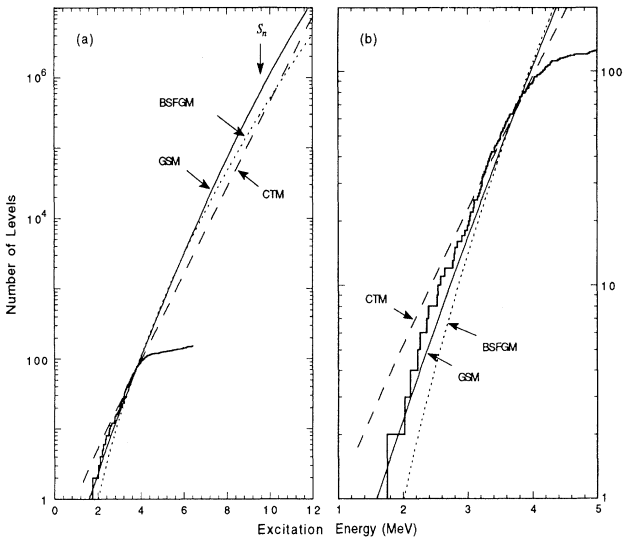

FIG. 3. Best two-parameter fits to the bound-state plus resonance data carried out with different level-density models. The parameters are $a=12.6$ MeV^{-1}, $E_1=1.45$ MeV for the BSFGM; $T=0.71$ MeV, $E_0=0.77$ MeV for the CTM; and $\tilde{a}=12.9$ MeV^{-1}, $\Delta_0=1.114$ MeV (fixed), $\delta_{\text{shift}}=0.67$ MeV for the GSM. For the BSFGM and the CTM, the spin-cutoff parameter σ^2 is taken as 15.1; for the GSM it is given by Eqs. (A2) and (A3).

IV. MICROSCOPIC GENERALIZED SUPERFLUID MODEL

A microscopic calculation of the level density for the single-particle schemes of the Woods-Saxon potential was also carried out following the methods outlined in Ref. [14]. The single-particle energies enter into the calculation of the necessary thermodynamic functions (including the energy and entropy) through a summation over the single-particle levels. A significant difference from the phenomenological version is that, in the microscopic model, the pairing-correlation function can be different for the neutron and proton subsystems. While requiring more input parameters, the microscopic approach treats closed-shell and near-closed-shell effects on the level density in a more individual fashion. Only vibrational enhancement was included here because ^{116}Sn is spherical, and the equations for calculating this enhancement were the same as those in the phenomenological description (see the Appendix). Because the proton shell is closed, the proton quasiparticle excitations can arise only at energies above 6 MeV. Below that energy the neutron quasiparticle excitations are dominant, but by themselves they would suggest a smaller level density than is observed experimentally. If the vibrational enhancement is included, then the comparison to experiment is much improved. The calculated curve runs almost parallel to the experimental data, but it is shifted to higher energy by about 0.3 MeV at low excitation energies and by 0.5 MeV at S_n [see the solid curve in Fig. 4(b)]. The microscopic calculations also reproduce quite well [see Fig. 4(a)] the limited data on the spin-cutoff parameter.

For comparison, the results of phenomenological calculations are shown in Figs. 4(a) and 4(b) as dashed curves. Compared to the results of the microscopic calculations (solid curves), the agreement with experiment is better for the level density and worse for the spin-cutoff parameter.

The $\tilde{a}(A)=11.8$-MeV^{-1} and $\Delta_0=1.22$-MeV values from the microscopic calculations are close to those from the phenomenological fits. Furthermore, the energy shift between the microscopic calculation and experiment is almost the same as that found in the phenomenological calculation. It may be that this shift simulates the rotational collective effects that were omitted in both calculations.

The possibility of such an explanation is connected with the well-known existence of quasirotational bands based on proton 2p-2h excitations. The lowest band built on the 0_2^+ state at 1.756 MeV was first discovered in $(\alpha,2n\gamma)$ reactions [19,20], and three higher-lying bands that had been predicted theoretically [21] have recently been identified [9]. A total of 14 such quasirotational states have now been identified up to 4.0 MeV, and they make a significant contribution to the total level density. To account for them in the GSM calculations, it would be necessary to include a rotational enhancement factor, but the formalism for enhancement caused by bands other than the ground-state band has not yet been developed.

If our interpretation of the supplementary energy shift

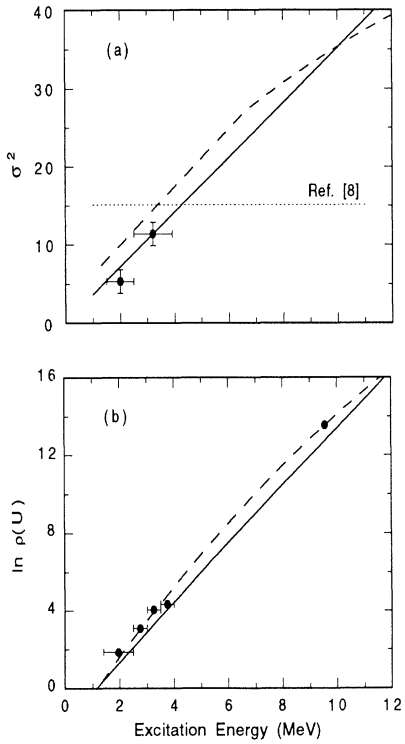

FIG. 4. Comparison of the (a) spin-cutoff factors σ^2 and (b) level densities $\rho(U)$ deduced from the data with those derived from the microscopic (solid curves) and the phenomenological versions of the GSM (dashed curves). The dotted line in (a) denotes the energy-independent value used in Ref. [8]. The solid curve in (b) includes the vibrational enhancement.

is correct, then the existence of an almost constant energy shift all the way up to S_n implies that the proton rotational enhancement is important to well above 10 MeV. Investigations of additional nuclei similar to ^{116}Sn (which has coexisting modes of excitation) will be of interest in the study of collective enhancement of level densities.

V. CONCLUSIONS

It has been shown that the phenomenological version of the GSM can successfully fit the bound-state level data of ^{116}Sn over a wide energy region and, at the same time, the level density at S_n. The best-fit parameters are in good agreement with those values determined from either theoretical considerations or systematics of fits to many other nuclei.

The BSFGM and the CTM are less successful in fitting simultaneously the level densities in the two energy regions. The BSFGM has two energy-independent parameters. When fitted to agree with the resonance data, this model gives a curve that has the wrong slope to ever agree in detail with the experimental bound-state staircase plot for this nucleus. Although the parameters of the CTM can be adjusted to fit the bound states alone quite well, these same parameters give an incorrect density in the resonance region.

The microscopic version of the GSM in its current form gives level densities in many nuclei that are systematically lower than the data by an almost constant factor. There are good reasons to believe that this deficiency results from the neglect of rotational collective effects. It is nevertheless satisfying that the parameters of the microscopic calculations are found to be similar to those from the phenomenological version.

The success of the GSM is attributed to the inclusion of many well-known characteristics of nuclear structure such as pairing correlations, shell structure, and collective excitations. The net result is that the level-density parameter a and the spin-cutoff parameter σ^2 become energy dependent, thus making this model more flexible in fitting level densities over a wide range of energy. The GSM expressions for the calculation of the level density are certainly more awkward than the simpler relations of the BSFGM and the CTM. However, this complication may be inescapable if the aim is to obtain a consistent description of the level density over a wide range of excitation energies for a large number of nuclei.

ACKNOWLEDGMENTS

We thank T. von Egidy and S. Grimes for helpful discussions. The current research was sponsored by the U.S. National Science Foundation under Grant No. PHY-9001465 to the University of Kentucky and by the U.S. Department of Energy under Contract No. DE-AC05-84OR21400 with Martin Marietta Energy Systems, Inc. (Oak Ridge).

APPENDIX

The density of quasiparticle excitations in Eq. (7) can be written in a form similar to the FGM:

$$\rho_{\rm qp}(U')=\frac{\exp(S)}{\sqrt{2\pi\sigma^2\,\det}}\ , \tag{A1}$$

where the effective excitation energy U' is defined in Eq. (9) and S is the entropy. In the GSM, the level density needs to be treated separately in two energy regions. These regions are separated by the critical temperature $t_{\rm cr}$ [see Eq. (8)]. At temperatures above $t_{\rm cr}$, the equations of state of the GSM differ [11,12] from the similar expressions of the FGM by a shift of excitation energy. In this region, the temperature, entropy, and other thermodynamic functions can be determined from U' using the equations

$$\begin{aligned} &U'=at^2+E_{\rm cond},\quad S=2at=2\sqrt{a(U'-E_{\rm cond})}\ ,\\ &\sigma^2=(6/\pi^2)a\langle m^2\rangle t,\quad \det=(144/\pi)a^3t^5\ , \end{aligned} \tag{A2}$$

where t is the thermodynamic temperature, $E_{\rm cond}$ is defined below, $\langle m^2\rangle=0.24\pm0.01A^{1/3}$ is the average square of the angular-momentum projection of the single-particle states near the Fermi surface, and the energy dependence of the parameter a is taken into account via Eq. (11).

To determine t, S, σ^2, and det from U' below the phase-transition point $t_{\rm cr}$, the simple parametrization proposed in Ref. [22] is used

$$\begin{aligned} &U'=U_{\rm cr}(1-\phi^2),\quad S=S_{\rm cr}(t_{\rm cr}/t)(1-\phi^2)\ ,\\ &\sigma^2=\sigma^2_{\rm cr}(1-\phi^2),\quad \det=\det_{\rm cr}(1-\phi^2)(1+\phi^2)^2\ . \end{aligned} \tag{A3}$$

The subscript cr denotes the values of the corresponding functions at the critical point, namely,

$$\begin{aligned} &U_{\rm cr}=a_{\rm cr}t^2_{\rm cr}+E_{\rm cond},\quad S_{\rm cr}=2a_{\rm cr}t_{\rm cr}\ ,\\ &\sigma^2_{\rm cr}=(6/\pi^2)a_{\rm cr}\langle m^2\rangle t_{\rm cr},\quad \det_{\rm cr}=(144/\pi)a^3_{\rm cr}t^5_{\rm cr}\ . \end{aligned} \tag{A4}$$

The relation between the function $\phi=[1-(U'/U_{\rm cr})]^{1/2}$ and temperature t is given by the equation

$$\phi=\tanh[(t_{\rm cr}/t)\phi]\ . \tag{A5}$$

From the solution of this equation, it is possible to find the temperature corresponding to a given excitation energy or, conversely, to find U' for a given $t<t_{\rm cr}$ and then use Eqs. (A3) to find the remaining functions. The condensation energy characterizing the decrease of the ground-state energy of the superfluid phase relative to the Fermi-gas phase is given by the expression

$$E_{\rm cond}=\frac{3}{2\pi^2}a_{\rm cr}\Delta_0^2\ , \tag{A6}$$

where Δ_0 is given by Eq. (15).

The influence of shell effects on the behavior of the thermodynamic functions in the superfluid phase, Eq. (A3), is reflected in the value of the level-density parameter $a_{\rm cr}$ at the critical point, which must be found by an iterative solution of the equation

$$a_{cr}=\tilde{a}\left\{1+\delta\varepsilon_0\frac{[1-\exp(-\gamma a_{cr}t_{cr}^2)]}{a_{cr}t_{cr}^2}\right\}, \quad \text{(A7)}$$

where $\delta\varepsilon_0$ and γ are the same quantities defined in Sec. III.

The vibrational enhancement of the level density can be written in the form

$$\kappa_{vibr}=\exp[\delta S-(\delta U/t)] , \quad \text{(A8)}$$

where δS and δU are changes in the entropy and excitation energy, respectively, resulting from the collective excitations. These changes are described by the relationships for a Bose gas:

$$\delta S=\sum_{i=0}^{\infty}(2\lambda_i+1)[(1+n_i)\ln(1+n_i)-n_i\ln(n_i)] \quad \text{(A9)}$$

and

$$\delta U=\sum_{i=0}^{\infty}(2\lambda_i+1)\omega_i n_i , \quad \text{(A10)}$$

where ω_i are the energies, λ_i the multipolarities, and n_i the occupation numbers for vibrational excitations at a given temperature. To account for the disappearance of collective enhancement of the level density at high temperatures, the occupation numbers were taken from[2]

$$n_i=\frac{\exp[-\gamma_i/(2\omega_i)]}{\exp[\omega_i/t]-1} , \quad \text{(A11)}$$

where γ_i are the spreading widths of the collective excitations. The spreading of vibrational excitations in nuclei is similar to the zero-sound damping in a Fermi liquid and the corresponding width can be written as

$$\gamma_i=C(\omega_i^2+4\pi^2t^2) . \quad \text{(A12)}$$

The value of $C=0.0075A^{1/3}$ MeV^{-1} was obtained from the systematics of the densities of low-lying levels and neutron resonances of medium-weight nuclei [12]. In that analysis, the measured values were employed for the energies of the first 2^+ states and $\hbar\omega=50A^{-2/3}$ MeV for the octupole excitations, whose influence is much weaker than the quadrupole ones.

The rotational enhancement factor (not used in the current work) can be written in the form [11]

$$\kappa_{rot}=\mathcal{I}_\perp t g(U)=\sigma_\perp^2 g(U)=\sigma^2(1+\tfrac{1}{3}\beta)g(U) , \quad \text{(A13)}$$

where $\mathcal{I}_\perp$ is the perpendicular moment of inertia and $g(U)$ is an empirical function that describes the damping of rotation in hot nuclei. An expression proposed by Hansen and Jensen [23] can be used for this function:

$$g(U)=\{1+\exp[(U-U_r)/d_r]\}^{-1}, \quad \text{(A14)}$$

where

$$U_r=120A^{1/3}\beta^2 \text{ MeV} \quad \text{(A15)}$$

and

$$d_r=1400A^{-2/3}\beta^2 \text{ MeV} . \quad \text{(A16)}$$

For nuclei with deformation parameters $\beta>0.2$, the damping of the rotation is negligible for energies below S_n. The uncertainty in $g(U)$ is then not very significant in the analysis of the bound levels and neutron resonances and $g(U)\approx 1$ for $U\le S_n$.

The flowchart of the computer program used to calculate the GSM level density is as follows. The input parameters are $\tilde{a}$, Δ_0, and δ_{shift}. The first quantity calculated is t_{cr} defined by Eq. (8). The implicit Eq. (A7) is then solved for a_{cr}. With E_{cond} given by Eq. (A6), all critical quantities defined in Eq. (A4) are then calculated. The thermodynamic temperature t corresponding to the excitation energy $U'\le U_{cr}$ is found from Eq. (A5). The quasiparticle density ρ_{qp} is obtained with Eqs. (A3) and (A1) when $U'<U_{cr}$ and with Eqs. (A2) and (A1) when $U'\ge U_{cr}$. The a value for use in Eq. (A2) is given by Eq. (11). The vibrational and rotational enhancements, κ_{vibr} and κ_{rot}, are calculated separately according to Eqs. (A8) and (A13), respectively. The three quantities, ρ_{qp}, κ_{vibr}, and κ_{rot} are multiplied together to obtain $\rho(U)$. The integrated number of levels (all spins and both parities) up to U is given by $\rho(U)$ multiplied by t. The density for a particular spin is obtained by multiplying $\rho(U)$ by $f(J)$ given by Eq. (3), with the crucial difference that σ^2, given by Eqs. (A2) and (A3), depends on the excitation energy.

[2]Some authors have defined n_i differently by omitting the factor 2 multiplying ω_i in the numerator of Eq. (A11). See, for instance, Eq. (7) of M. I. Svirin and G. N. Smirenkin, Yad. Fiz. **48**, 682 (1988) [Sov. J. Nucl. Phys. **48**, 437 (1989)].

[1] H. A. Bethe, Phys. Rev. **50**, 332 (1936); Rev. Mod. Phys. **9**, 69 (1937).

[2] T. Ericson, Nucl. Phys. **11**, 481 (1959); Adv. Phys. **9**, 425 (1960).

[3] A. Gilbert, F. S. Chen, and A. G. W. Cameron, Can. J. Phys. **43**, 1248 (1965).

[4] A. Gilbert and A. G. W. Cameron, Can. J. Phys. **43**, 1446 (1965).

[5] E. Gadioli and L. Zetta, Phys. Rev. **167**, 1016 (1968); J. R. Huizenga, H. K. Vonach, A. A. Katsanos, A. J. Gorski, and C. J. Stephan, *ibid.* **182**, 1149 (1969); H. Vonach and M. Hille, Nucl. Phys. **A127**, 289 (1969).

[6] W. Dilg, W. Schantl, H. Vonach, and M. Uhl, Nucl. Phys. **A217**, 269 (1973).

[7] T. von Egidy, A. N. Behkami, and H. H. Schmidt, Nucl. Phys. **A454**, 109 (1986).

[8] T. von Egidy, H. H. Schmidt, and A. N. Behkami, Nucl. Phys. **A481**, 189 (1988).

[9] S. Raman, T. A. Walkiewicz, S. Kahane, E. T. Jurney, J. Sa, Z. Gácsi, J. L. Weil, K. Allaart, G. Bonsignori, and J.

F. Shriner, Jr., Phys. Rev. C **43**, 521 (1991).
[10] V. M. Timokhov, M. V. Bokhovko, A. G. Isakov, L. E. Kazakov, V. N. Kononov, G. N. Manturov, E. D. Poletaev, and V. G. Pronyaev, Yad. Fiz. **50**, 609 (1989) [Sov. J. Nucl. Phys. **50**, 375 (1989)].
[11] A. V. Ignatyuk, K. K. Istekov, and G. N. Smirenkin, Yad. Fiz. **29**, 875 (1979) [Sov. J. Nucl. Phys. **29**, 450 (1979)].
[12] O. T. Grudzevich, A. V. Ignatyuk, V. I. Plyaskin, and A. V. Zelenetsky, in *Proceedings of the International Conference on Nuclear Data for Science and Technology, Mito, 1988,* edited by S. Igarasi (Saikon, Tokyo, 1988), p. 767.
[13] J. R. Huizenga and L. G. Moretto, Annu. Rev. Nucl. Sci. **22**, 427 (1972).
[14] A. V. Ignatyuk, *Statistical Properties of Excited Atomic Nuclei* (Energoatomizdat, Moscow, 1983), translated as International Atomic Energy Agency Report INDC(CCP)-223/L, 1985; A. V. Ignatyuk and Yu. N. Shubin, Yad. Fiz. **8**, 1135 (1968) [Sov. J. Nucl. Phys. **8**, 660 (1969)]; A. V. Ignatyuk, Yu. V. Sokolov, and Yu. N. Shubin, *ibid.* **18**, 989 (1973) [**18**, 510 (1974)].
[15] S. F. Mughabghab, M. Divadeenam, and N. E. Holden, *Neutron Cross Sections* (Academic, New York, 1981), Vol. 1, Part A.
[16] G. Reffo, in Proceedings of the Course on Nuclear Theory for Applications, Trieste, 1980, International Atomic Energy Agency Report IAEA-SMR-43, 1980, p. 205.
[17] V. S. Ramamurthy, S. K. Kataria, and S. S. Kapoor, in Proceedings of the IAEA Advisory Group Meeting on Basic and Applied Problems of Nuclear Level Densities, Brookhaven, 1983, Brookhaven National Laboratory Report BNL-NCS-51964, 1983, p. 187.
[18] W. D. Myers, *Droplet Model of Atomic Nuclei* (IFI/Plenum, New York, 1977).
[19] J. Bron, W. H. A. Hesselink, A. van Poelgeest, J. J. A. Zalmstra, M. J. Uitzinger, H. Verheul, K. Heyde, M. Waroquier, H. Vincx, and P. van Isacker, Nucl. Phys. **A318**, 335 (1979).
[20] A. van Poelgeest, J. Bron, W. H. A. Hesselink, K. Allaart, J. J. A. Zalmstra, M. J. Uitzinger, and H. Verheul, Nucl. Phys. **A346**, 70 (1980).
[21] G. Wenes, P. Van Isacker, M. Waroquier, K. Heyde, and J. Van Maldegham, Phys. Rev. C **23**, 2291 (1981).
[22] A. V. Ignatyuk and Yu. N. Shubin, Izv. Akad. Nauk SSSR, Ser. Fiz. **37**, 1947 (1973) [Bull. Acad. Sci., USSR, Phys. Ser. **37**, 127 (1973)].
[23] G. Hansen and A. S. Jensen, Nucl. Phys. **A406**, 236 (1983).